Biochimica et Biophysica Acta 1857 (2016) 1943–1948

Contents lists available at ScienceDirect

Biochimica et Biophysica Acta

journal homepage: www.elsevier.com/locate/bbabio

Corrigendum to "Influence of Histidine-198 of the D1 subunit on the properties of the primary electron donor, P_{680}, of photosystem II in *Thermosynechococcus elongatus*"

Miwa Sugiura [a,*], Yui Ozaki [a], Fabrice Rappaport [b,1], Alain Boussac [c]

[a] Proteo-Science Research Center, Ehime University, Bunkyo-cho, Matsuyama, Ehime 790-8577, Japan
[b] Institut de Biologie Physico-Chimique, UMR 7141 CNRS and Université Pierre et Marie Curie, 13 rue Pierre et Marie Curie, 75005 Paris, France
[c] iBiTec-S, SB2SM, CNRS UMR 9198, CEA Saclay, 91191 Gif-sur-Yvette, France

ARTICLE INFO

Article history:
Received 29 August 2016
Received in revised form 26 September 2016
Accepted 28 September 2016
Available online 2 October 2016

Keywords:
Photosystem II
P_{680}
Electron transfer
Chlorophyll *a* axial ligand
Site-directed mutagenesis
Thermosynechococcus elongatus

ABSTRACT

Two mutants, D1-H198Q and D1-H198A, have been previously constructed in *Thermosynechococcus elongatus* with the aim at modifying the redox potential of the $P_{680}^{\bullet+}/P_{680}$ couple by changing the axial ligand of P_{D1}, one the two chlorophylls of the Photosystem II primary electron donor [Sugiura et al., Biochim. Biophys. Acta 1777 (2008) 331–342]. However, after the publication of this work it was pointed out to us by Dr. Eberhard Schlodder (Technische Universität Berlin) that in both mutants the pheophytin band shift which is observed upon the reduction of Q_A was centered at 544 nm instead of 547 nm, clearly showing that the D1 protein corresponded to PsbA1 whereas the mutants were supposedly constructed in the *psbA*$_3$ gene so that the conclusions in our previous paper were wrong. O_2 evolving mutants have been therefore reconstructed and their analyze shows that they are now correct mutants which are suitable for further studies. Indeed, the D1-H198Q mutation downshifted by ≈3 nm the $P_{680}^{\bullet+}/P_{680}$ difference absorption spectrum in the Soret region and increased the redox potential of the $P_{680}^{\bullet+}/P_{680}$ couple and the D1-H198A mutation decreased the redox potential of the $P_{680}^{\bullet+}/P_{680}$ couple all these effects being comparable to those which were observed in *Synechocystis* sp. PCC 6803 [Diner et al., Biochemistry 40 (2001) 9265–9281 and Merry et al. Biochemistry 37 (1998) 17,439–17,447]. We apologize for having presented wrong data and wrong conclusions in our earlier publication.

1. Introduction

The light-driven oxidation of water in Photosystem II (PSII) is a key step in photosynthesis, the process that is the main input of energy into biology and is thus responsible not only for the production of biomass including food, fibre and fuels (fossil and non-fossil) but also putting O_2 into the atmosphere. PSII in cyanobacteria is made up of 17 membrane proteins and 3 extrinsic proteins. Altogether these 20 subunits bear 35 chlorophylls, 2 pheophytins (Phe), 2 hemes, 1 non-heme iron, 2 plastoquinones (Q_A and Q_B), a Mn_4CaO_5 cluster, 2 Cl^-, 12 carotenoids and 25 lipids [1,2].

The excitation resulting from the absorption of a photon is transferred to the photochemical trap P_{680}, which is composed of four chlorophyll *a* molecules, P_{D1}/P_{D2} and Chl_{D1}/Chl_{D2}, and two pheophytin *a* molecules, Phe_{D1}/Phe_{D2}. Charge separation then occurs. After some picoseconds the positive charge is mainly stabilized on P_{D1} but this is often termed P_{680}^{+}. P_{680}^{+} then oxidizes Y_Z, the Tyr161 of the D1 polypeptide, which in turn oxidizes the Mn_4CaO_5 cluster. On the electron acceptor side, the electron is transferred to the primary quinone electron acceptor, Q_A, and then to Q_B, a two-electron and two-proton acceptor, *e.g.* [3–5] for reviews. The Mn_4CaO_5 cluster accumulates oxidizing equivalents and acts as the catalytic site for water oxidation. The enzyme cycles sequentially through five redox states denoted S_n where *n* stands for the number of stored oxidizing equivalents. Upon formation of the S_4 state two molecules of water are rapidly oxidized, the S_0 state is regenerated and O_2 is released, *e.g.* [5–9].

A consensus has emerged that primary charge separation in PSII occurs between Chl_{D1} and $Pheo_{D1}$, *e.g.* [10,11]. In a few ps, the $P_{680}^{\bullet+}Pheo_{D1}^{\bullet-}$ state is then formed with 80% of the cation residing on P_{D1} and 20% on P_{D2} [3], see also [12] for similar calculated values based on the recent high-resolution PSII structure [1]. Then, the pheophytin anion transfers the electron to the quinone, Q_A. P_{680}^{+} is reduced by Tyr_Z, at position 161 of the D1 protein. $Tyr_Z^{\bullet}$ is in turn reduced by the Mn_4CaO_5 cluster.

Abbreviations: PSII, Photosystem II; Chl, chlorophyll; MES, 2–(*N*–morpholino) ethanesulfonic acid; P_{680}, chlorophyll dimer acting as the second electron donor; Q_A, primary quinone acceptor; Q_B, secondary quinone acceptor; 43H, *T. elongatus* strain with a His–tag on the C terminus of CP43; WT*3, cells containing only the *psbA*$_3$ gene; $Pheo_{D1}$, pheophytin; P_{D1} and P_{D2}, Chl monomer of P_{680} on the D1 or D2 side, respectively; E_m, redox potential *versus* SHE; TL, Thermoluminescence; DCMU, 3–(3,4–dichlorophenyl)–1,1–dimethylurea; PPBQ, phenyl *p*–benzoquinone; DCBQ, 2,6 dichloro-1,4 benzoquinone; β–DM, *n*–dodecyl–β–maltoside; Cm, chloramphenicol; Gm, gentamycin; Sm, streptomycin; Sp, spectinomycin.

* Corresponding author.
E-mail address: miwa.sugiura@ehime-u.ac.jp (M. Sugiura).

[1] Deceased before the end of this work.

http://dx.doi.org/10.1016/j.bbabio.2016.09.012
0005-2728/

An extraordinary feature of PSII amongst reaction centre complexes is the high redox potential of the $P^{\bullet+}_{680}/P_{680}$ couple which is required to drive water oxidation, *e.g.* [13]. Possible reasons for the elevated value compared to Chl*a in vitro* include protein-pigment interactions, such as H-bonding, *e.g.* [12,14–16], pigment-cofactor interactions [17–21], a low dielectric environment [22] and puckering of pigment molecules [23].

The importance of the amino-acid ligand, D1-His198, on the functional properties of P_{D1} has been examined by mutagenesis in the mesophilic cyanobacterium *Synechocyctis* sp. PCC 6803 [10]. Of the 11 mutants examined only 3 were found to be photoautotrophic: H198Q, H198A and H198C mutants. Interestingly, in the D1-H198A mutant the Mg atom was conserved despite the lack of any proteinaceous ligand. The likely substitution of the His ligand by a water molecule had nevertheless some influence on the $P^{\bullet+}_{680}/P_{680}$ absorption difference spectrum which was down-shifted by ≈2 nm in the Soret region. This spectroscopic change was accompanied by a decrease of ≈80 mV in the estimated mid-point redox potential of the $P^{\bullet+}_{680}/P_{680}$ couple. In the D1-H198Q mutant, in which glutamine could possibly act as a ligand to Mg, the $P^{\bullet+}_{680}/P_{680}$ absorption difference spectrum was downshifted by 3–4 nm in the Soret region but the redox potential was almost unchanged in PSII core complexes. Thus, the correlation between the spectral changes and the redox properties of P_{680} were not obvious in these mutants [10]. This prompted us to study the role of the D1 axial ligand to P_{D1} in the thermophilic cyanobacterium *Thermosynechococcus elongatus* from which fully active PSII can be purified and importantly for which the PSII structure likely identical to that one of *T. vulcanus* is known [1,2]. To achieve this aim we have described the development of a mutagenesis system for the construction of D1 mutants in *T. elongatus* and the characterization of D1-H198Q and D1-H198A mutants by low-temperature fluorescence, thermoluminescence, oxygen-evolution, FTIR spectroscopy and time-resolved absorption spectroscopy has been reported [24].

The two mutants, D1-H198Q and D1-H198A, were constructed in a strain (WT*3) in which the *psbA*$_1$ and *psbA*$_2$ gene were previously deleted so that this strain expressed only the *psbA*$_3$ gene. However, after the publication of this earlier work [24] and in order to investigate the Qy region of the $P^{\bullet+}_{680}/P_{680}$ difference spectra, it was observed by Eberhard Schlodder from the Technische Universität in Berlin (Max Volmer Lab, Str 17 Juni 135, D-10623 Berlin, Germany) that in both mutants the pheophytin band shift which is observed upon the reduction of Q_A was centered at 544 nm instead of 547 nm clearly showing that the D1 protein corresponded to PsbA1 whereas the mutants were constructed in the *psbA*$_3$ gene. The red shift by ≈3.0 nm of the C550 band–shift for the PsbA3–PSII sample, relative to the PsbA1–PSII sample, reflects the stronger hydrogen bond to the ^{1}13–keto of the $Pheo_{D1}$ from the carboxylate group of E130 in PsbA3–PSII than from Q130 in PsbA1–PSII, as previously shown [25,26].

Since to determine at which step the contamination of the strains occurred in our earlier work was impossible we decided to reconstruct the two mutants and to redo the most important experiments with new control experiments in order to add a *corrigendum* on our previous conclusions instead of presenting a simple retraction.

2. Materials and methods

The site-directed mutant strains PsbA3/H198A and PsbA3/H198Q were reconstructed from *T. elongatus* 43-H cells [27]. First, site-directed mutations were done in the *psbA*$_3$ gene in the 43H strain, *i.e.* in the strain which contains the three *psbA* genes, by using a spectinomycine (Sp)/streptomycine (Sm) resistant cassette in a site-directed plasmids as described in [24]. Segregation of all the *psbA*$_3$ copies in genome was confirmed by digestion of *psbA*$_3$ with *Pvu* II after PCR amplification of the mutated region by using the *P3* (5′- CCAGGCACTCA ACTGGAGTTGTGAACGGTT -3′) and *P4* primers (5′ CCACCGAAACCGAA TCTGCCAACTACGGTT −3′) (Fig. 1).

Then, both the H198A and H198Q mutants were knocked out by substitution of gentamycine (Gm) resistant cassette and chloramphenicol (Cm) resistant cassette for the *psbA*$_1$ - *psbA*$_2$ genes, respectively. Fully segregated *psbA*$_1$/*psbA*$_2$-deletion mutants were selected by growth on either Gm or Cm for H198A and H198Q, respectively. Their genotype were confirmed by PCR analysis using the *P1* primer (5′ GGGCACCACTC GAATGGTTTGCTCGTGG −3′) and *P2* primer (5′ ACCTCTCTAGTGATAA GTAGTGATAAGTCC −3′) as shown in Fig. 1A and D. Plasmid DNA were introduced into *T. elongatus* cells by electroporation (BioRad gene pulser). The segregated cells were selected as single colonies on DTN agar plates containing 25 μg Sp mL^{-1}, 10 μg Sm mL^{-1}, 40 μg Km mL^{-1} and 5 μg Cm mL^{-1}.

Cells were cultivated and the PSII complexes were purified as previously described [28]. Absorption changes were measured with a lab–built spectrophotometer [29] where the absorption changes are sampled at discrete times by short analytical flashes. These analytical flashes were provided by an optical parametric oscillator pumped by a neodymium:yttrium–aluminum garnet laser (Nd:YAG, 355 nm), which produces monochromatic flashes (1 nm full–width at half–maximum) with a duration of 5 ns. Actinic flashes were provided by a second neodymium:yttrium–aluminum garnet laser (Nd:YAG, 532 nm), which pumped an optical parametric oscillator producing monochromatic saturating flashes at 695 nm (1 nm full–width at half–maximum) with a duration of 5 ns. The path length of the cuvette was 2.5 mm. PSII was used at 25 μg of Chl mL^{-1} in 1 M betaine, 15 mM $CaCl_2$, 15 mM $MgCl_2$, and 40 mM MES (pH 6.5). PSII were dark–adapted for ≈1 h at room temperature (20–22 °C) before the addition of 0.1 mM phenyl *p*–benzoquinone (PPBQ) dissolved in dimethyl sulfoxide.

Thermoluminescence (TL) glow curves were measured with a lab–built apparatus [30,31]. PSII core complexes were diluted to 10 μg Chl mL^{-1} in 1 M betaine, 40 mM MES, 15 mM $MgCl_2$, 15 mM $CaCl_2$, pH 6.5 and then dark–adapted for 1 h at room temperature. Before loading the sample, 50 μM DCMU were added to the dark–adapted samples. The samples were illuminated at 0 °C by using a saturating xenon flash. Immediately after the flash, the samples were heated at the constant heating rate indicated in the legend of the figure and TL emission was detected. It was checked that, after dilution, the 3 PSII samples had a similar OD at 673 nm.

The O_2 activity was measured at 25 °C by using a Clark type oxygen electrode (Hansatech) with continuous saturating white light through infrared and water filters. The activity was measured over a period of 1.5 min in the presence of 0.5 mM 2,6–dichloro–*p*–benzoquinone (dissolved in dimethyl sulfoxide) as an electron acceptor.

Cw-EPR spectra were recorded using a standard ER 4102 (Bruker) X-band resonator with a Bruker Elexsys 500 X-band spectrometer equipped with an Oxford Instruments cryostat (ESR 900). The PSII samples at 1.1 mg of Chl mL^{-1} were loaded in the dark into quartz EPR tubes and further dark-adapted for 1 h at room temperature. Then, the samples were frozen in the dark to 198 K and then transferred to 77 K in liquid N_2. Illuminations with visible light for approximately 5–10 s with a 800 W tungsten lamp filtered by water and infrared cut-off filters at temperatures close to 200 K were done in a non-silvered dewar in ethanol cooled down with dry ice. No artificial electron acceptors were added to probe the redox state of the PSII electron acceptor side. Prior to the measurements all the samples were degassed at 198 K.

3. Results and discussion

3.1. Intactness of the mutant PSII

D1-H198Q and D1-H198A PSII core complexes exhibited an O_2 evolving activity of ≈3300 μmol O_2 (mg Chl)$^{-1}$ h^{-1} and ≈3000 μmol O_2 (mg Chl)$^{-1}$ h^{-1}, respectively, thus confirming that these mutations did not affect the formation of a PSII with a high activity. The EPR results shown in Fig. 2 also show that the S_2 multiline signal induced by 200 K

illumination had an amplitude similar in the WT*3 PSII and in the two mutants thus showing that S_2 can be formed in the same proportion of centers in the three samples. The amplitude of the $Q_A^- Fe^{2+} Q_B^-$ signal at g = 1.66 (≈4000–4200 gauss) [32] induced by the 200 K illumination was also similar in the two mutants thus showing that the amount of $Q_A Fe^{2+} Q_B^-$ prior to the illumination was similar. The addition of DCMU in the dark-adapted mutants was therefore not expected to result in a different proportion of closed centers in the $Q_A^- Fe^{2+}$/DCMU state prior to the flash illumination in the thermoluminescence experiment (see below).

3.2. Time-resolved flash-induced absorption changes around 550 nm

Fig. 3 shows the electrochromic blue shift undergone by $Pheo_{D1}$ upon reduction of Q_A and known as the C–550 bandshift in PsbA1–PSII (green trace), PsbA3–PSII (black trace) and PsbA3/H198Q–PSII (red trace). For these measurements, the samples were first dark–adapted for 1 h at room temperature then, the absorption changes were measured 15 μs after each actinic flash in a series. The data shown in Fig. 3 are the average of the individual absorption changes induced by the 2nd to 7th flashes. The red shift by ≈3.0 nm of the C550

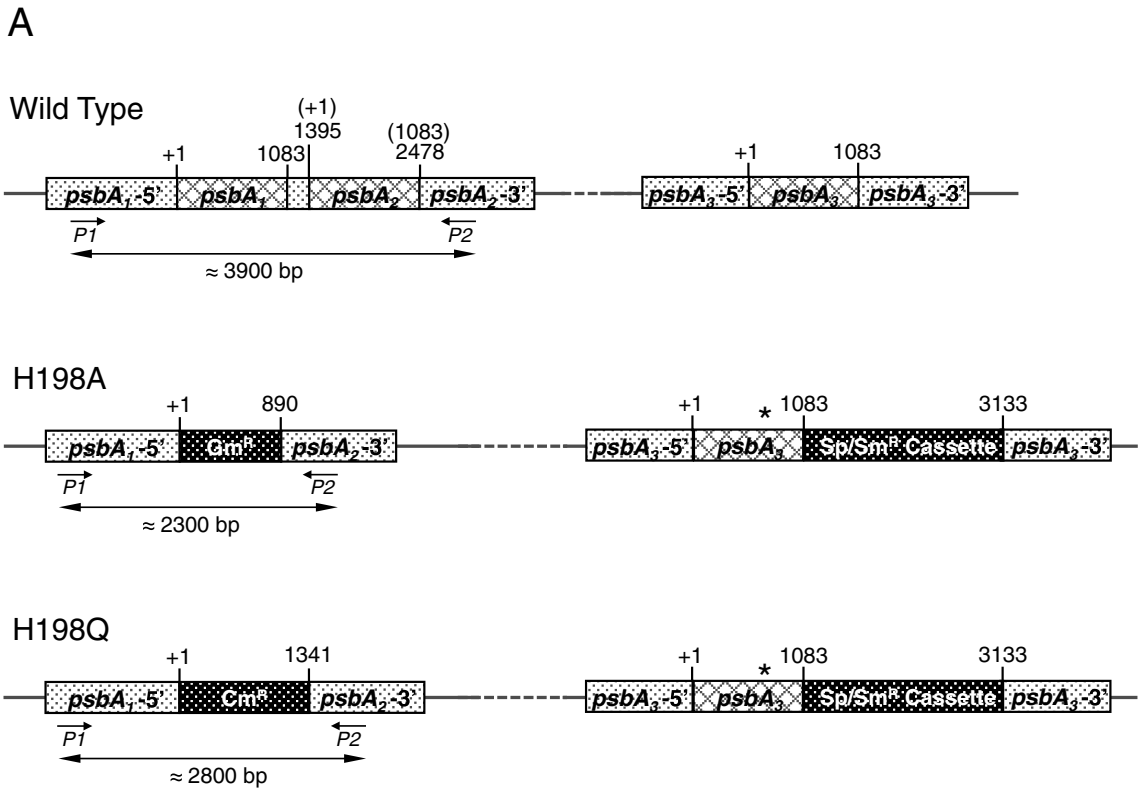

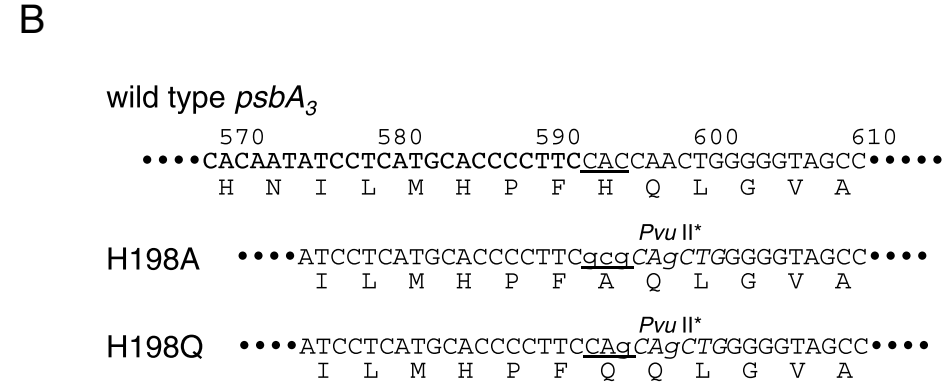

Fig. 1. (A) Map around the $psbA_1$ - $psbA_2$ genes and $psbA_3$ gene in wild type and H198A and H198Q mutants. For deletion of both the $psbA_1$ and $psbA_2$ genes, Gm resistant cassette and Cm resistant cassette were substituted in H198A and H198Q, respectively. Site-directed mutations were introduced in $psbA_3$ (asterisks) with Sp/Sm resistant cassette. *P1* and *P2* show positions of PCR primers to confirm the length of the $psbA_1$ and $psbA_2$ genes and/or the Gm and Cm resistant cassettes. (B) The nucleotides and translated amino acids sequences of PsbA3 of wild type, H198A and H198Q including amino acid at position 198. Newly created restriction enzyme sites for site-directed mutations are shown in italic. *Pvu* II sites were newly created for both mutants. (C) Physical map around $psbA_3$ and theoretical DNA length after treating with *Pvu* II the PCR products by using primers *P3* and *P4*. The created *Pvu* II (shown as *Pvu* II*) sites for H198A and H198Q mutants are at position + 595. As $psbA_3$ of wild type has Pvu II at position + 54, digestion of products from the mutants with *Pvu* II generated fragments at 124-bp, 541-bp, and 278-bp. (D) (a) Agarose gel (1%) electrophoresis of PCR amplification products using the *P1* and *P2* primers. Lanes 1 and 6, 1 kb DNA ladder markers (Nacalai Tesque, Japan); lane 2, 43-H strain; lane 3, WT*3 (Δ$psbA_1$/Δ$psbA_2$/43-H) strain; lane 4, H198A strain; lane 5, H198Q strain. (b) Agarose gel (2%) electrophoresis of PCR products using the *P3* and *P4* primers (lanes 2, 4 and 6) and the products after digestion with *Pvu* II (lanes 3, 5 and 7). Lanes 1 and 6, 100 bp DNA ladder markers (Nacalai Tesque, Japan); lanes 2 and 3, WT*3 strain; lanes 4 and 5, H198A strain; lanes 6 and 7, H198Q strain.

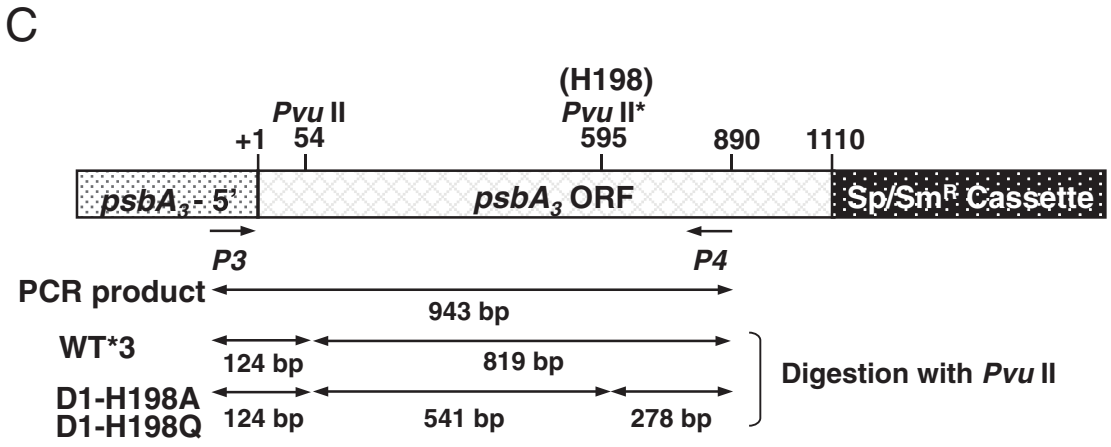

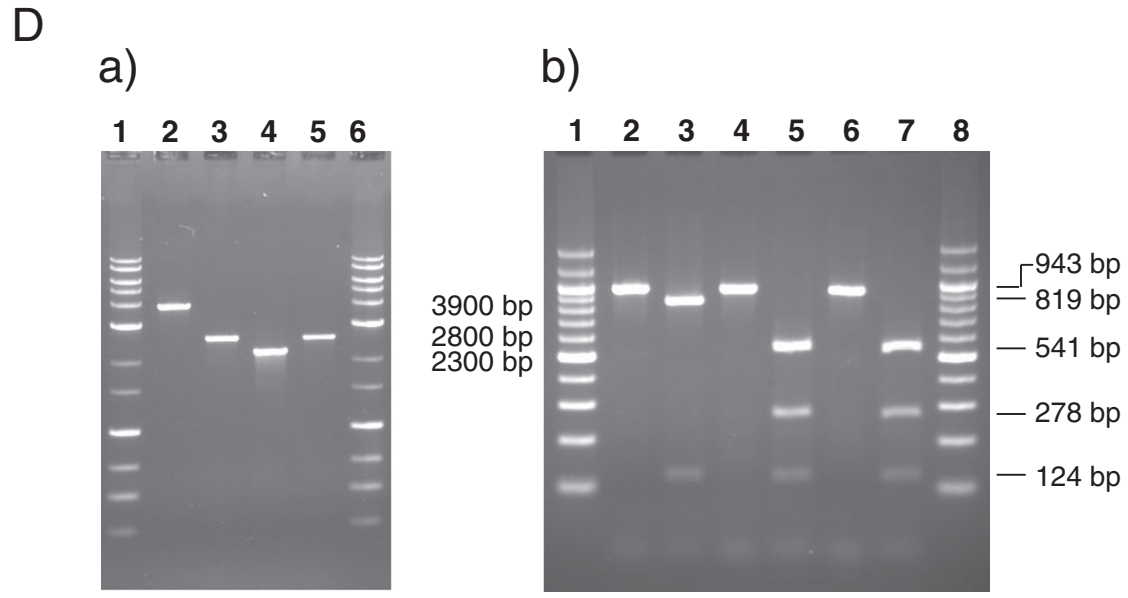

Fig. 1 (*continued*).

band–shift for the PsbA3–PSII sample, relative to the PsbA1–PSII sample, reflects the stronger hydrogen bond to the ^{1}13–keto of the $Pheo_{D1}$ from the carboxylate group of E130 in PsbA3–PSII than from Q130 in PsbA1–PSII, as previously shown [25,26,28]. In the PsbA3/H198Q–PSII sample the electrochromic bandshift was similar to that in the PsbA3–PSII sample, showing that in this PSII mutant D1 corresponded to PsbA3. Because of the death of our colleague Fabrice Rappaport we could not do the time-resolved flash-induced absorption changes measurements in the D1-H198A mutant. However, as shown below, this mutant has been probed by thermoluminescence experiment.

3.3. Time-resolved flash-induced absorption changes around 430 nm

In this spectral region, the redox changes of several species, such as the Chls, cytochromes, Tyr_Z and Q_A are associated with absorption changes. The most prominent one, however, is associated with the formation of $P^{\bullet+}_{680}$. The $P^{\bullet+}_{680}/P_{680}$ difference spectrum exhibits a strong Soret band bleaching in the 430 nm region. Fig. 4 shows the absorption changes from 411 to 455 nm in PsbA3-PSII and in the PsbA3/H198Q PSII mutant. The absorption changes were measured 15 ns after the first flash, given to dark-adapted PSII *i.e.* in the S_1-state, and corresponded to the $P_{680}Q_A$ to $P^{\bullet+}_{680}Q^{\bullet-}_A$ transition. The O_2 evolving D1-H198Q PSII mutant exhibited a blue shift by about 3–4 nm exactly as observed in *Synechocystis* sp. PCC 6803 [10].

3.4. Energetic effects of the D1-H198 mutations in O_2 evolving PSII

A change in the redox potential of the $P^{\bullet+}_{680}/P_{680}$ couple can be assessed with thermoluminescence experiments by measuring the glow curve [33–36] originating from the $S_2Q^{\bullet-}_A$ charge recombination in the presence of DCMU (Q band). Fig. 5 shows the thermoluminescence glow curve, in the presence of DCMU, resulting from the $S_2Q^{-}_A$ recombination recorded in PsbA3-PSII (black trace), PsbA3/H198A PSII (blue trace) and PsbA3/H198Q PSII (red trace).

In the D1-H198Q mutant, the glow curve was larger than in WT*3 PSII and the peak of the glow curve was up-shifted by ≈6 °C from 27 °C to 33 °C. This phenotype is in a good agreement with what is expected for a more positive $P^{\bullet+}_{680}/P_{680}$ redox couple [36]. Indeed, in conditions where only the E_m of the $P^{\bullet+}_{680}/P_{680}$ couple varies, a more positive E_m value is expected to translate into a higher peak temperature, owing to a larger energy gap between the $S_2Tyr_ZP_{680}$ and the $S_1Tyr_ZP^{\bullet+}_{680}$ pairs and a larger intensity of the TL glow curve owing to a

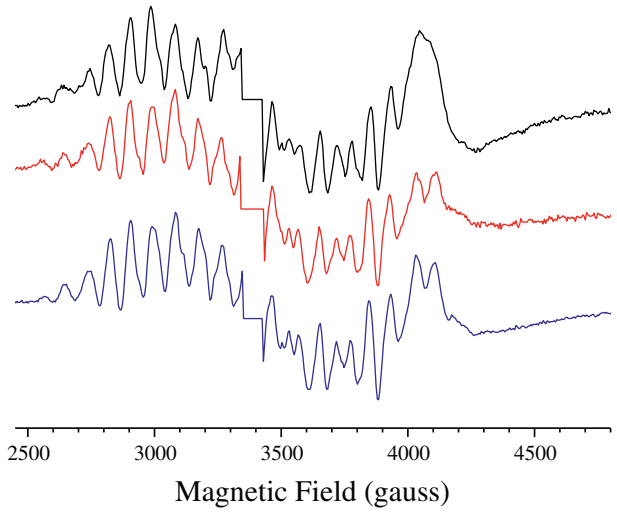

Fig. 2. Light-*minus*-dark EPR spectra induced by 200 K illumination of dark-adapted PsbA3-PSII (black spectrum), PsbA3/H198Q PSII (red spectrum) and PsbA3/H198A PSII (blue spectrum). PSII concentration = 1.1 mg Chl mL^{-1}. Instrument settings: modulation amplitude, 25 gauss; microwave power, 20 mW; microwave frequency, 9.4 GHz; modulation frequency, 100 kHz. Temperature, 8.6 K. It was checked that the reaction center concentrations were similar by using the $Tyr_D^{\bullet}$ EPR signal as a probe. The spectral region corresponding to the $Tyr_D^{\bullet}$ EPR signal has been deleted.

smaller free energy gap between P_{680}*Pheo and $P_{680}^{\bullet+}Pheo^{\bullet-}$, see [32–34] for a detailed explanation of the TL glow curve dependence upon changes of the various energy level of the radical pairs involved in luminescence. From kinetics of the charge recombination it has been estimated earlier [10] that the E_m of the $P_{680}^{\bullet+}/P_{680}$ couple in the H198Q mutant was found ≈50 mV higher than in the wildtype whole cells but almost unchanged in PSII core complexes. This difference was attributed to the loss of the Mn_4 cluster in the PSII core complexes in the mutant [10]. Here, with active H198Q PSII and according to the empirical relationship between the shift in free energy and the peak temperature discussed in [35,36], the expected upshift in the E_m of the $P_{680}^{\bullet+}/P_{680}$ couple resulting from the H198Q single site directed mutation in PsbA3–PSII would be ≈15 mV. This value is very close to that one found by Merry et al. [37] who found the $P_{680}^{\bullet+}/P_{680}$ couple to be more positive by 13–19 mV in the D1-H198Q mutant.

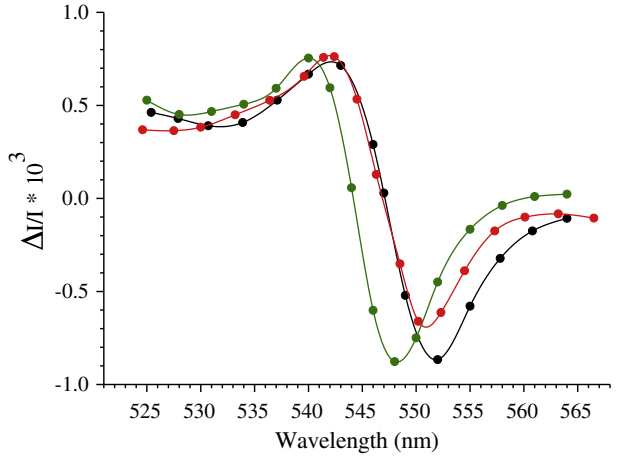

Fig. 3. Light–induced difference spectra around 545 nm. The flash–induced absorption changes were measured in PsbA1–PSII (green trace), PsbA3–PSII (black trace) and PsbA3/H198Q–PSII (red trace). Measurements were performed 15 μs after the flash and were averaged from the 2nd to 7th flash given to dark–adapted PSII. Upon dark–adaptation for 1 h at room temperature, 100 μM PPBQ (dissolved in dimethyl sulfoxide) was added to the samples (Chl concentration was 25 μg mL^{-1}). The difference spectra were approximately normalized to the same amplitude.

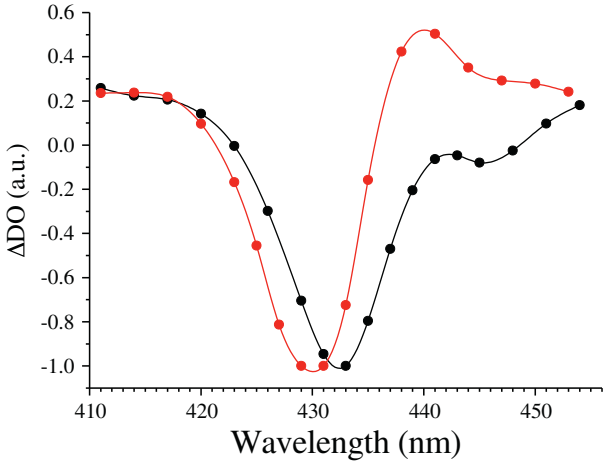

Fig. 4. Flash-induced absorption changes were measured in PsbA3-PSII (black trace) and PsbA3/H198Q PSII (red trace) 15 ns after the first flash given on dark-adapted PSII. Upon dark-adaptation for 1 h at room temperature, 100 μM PPBQ (dissolved in dimethylsulfoxide) was added to the samples with Chl = 25 μg mL^{-1}.

The situation in the D1-H198A mutant is more complex to analyze. In the two previous studies [10,37], the $P_{680}^{\bullet+}/P_{680}$ couple was estimated to be less positive by 23–29 mV in [37] and less positive by 74–84 mV in [10]. In the most simple case, a decrease in the E_m of the $P_{680}^{\bullet+}/P_{680}$ couple would translate into a lower peak temperature owing to a smaller energy gap between the $S_2Tyr_ZP_{680}$ and the $S_1Tyr_ZP_{680}^{\bullet+}$ pairs and a lower intensity of the TL glow curve owing to a larger free energy gap between P_{680}*Pheo and $P_{680}^{\bullet+}Pheo^{\bullet-}$ [36]. However, as detailed in [36], a mutation in a ligand of P_{680} could also affect the energy level of P_{680}* so that the three routes for a charge recombination (the direct, indirect and radiative routes) could be affected. Although, a change in the E_m of the $P_{680}^{\bullet+}/P_{680}$ couple in active H198A-PSII has been observed [10,37] and therefore cannot be excluded, from all the theoretical cases investigated in [36] an increase in the energy level of P_{680}* in the D1-H198A mutant would be the major effect to explain the TL data. It should be mentioned that TL measurements in whole cells in *Synechocystis* sp. PCC 6803 also showed a decrease of the TL amplitude in the H198A mutant and an increase in the TL amplitude in the H198Q mutant [35].

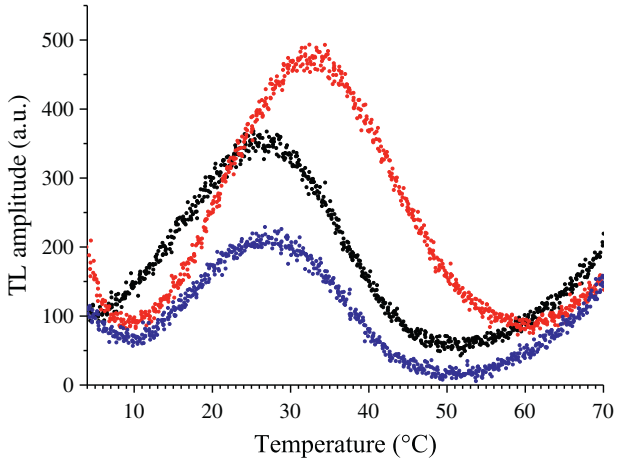

Fig. 5. Thermoluminescence glow curves from $S_2Q_A^{-\bullet}$ charge recombination formed by 1 flash at 0 °C in the presence of DCMU (50 μM) in PsbA3–PSII (black trace),PsbA3/H198Q–PSII (red trace) and PsbA3/H198A–PSII (blue trace). Concentration, 10 μg Chl mL^{-1}. Heating rate, 0.3 °C/s. See Materials and Methods for other details.

4. Conclusion

In this work, the two mutants, D1-H198Q and D1-H198A, which have been previously constructed in *Thermosynechococcus elongatus* with the aim to modify the redox potential of the P^{+}_{680}/P_{680} couple by changing the axial ligand of P_{D1}, one the two chlorophylls of the primary electron donor [24], have been reconstructed. The characterization of these new mutants presented above shows that our previous conclusions were wrong and that these new O_2 evolving mutants exhibit a correct phenotype which makes them suitable for further studies.

Transparency document

The Transparency document associated with this article can be found, in online version.

Acknowledgements

Jean-Marc Ducruet is acknowledged for his help in setting up a new TL set up. We thank to Makoto Nakamura (Ehime University) for technical assistance.

References

[1] Y. Umena, K. Kawakami, J.-R. Shen, N. Kamiya, Crystal structure of oxygen–evolving photosystem II at a resolution of 1.9 Å, Nature 473 (2011) 55–60.
[2] M. Suga, F. Akita, K. Hirata, G. Ueno, H. Murakami, Y. Nakajima, T. Shimizu, K. Yamashita, M. Yamamoto, H. Ago, J.-R. Shen, Native structure of photosystem II at 1.95 Å resolution viewed by femtosecond X-ray pulses, Nature 517 (2015) 99–103.
[3] B.A. Diner, F. Rappaport, Structure, dynamics, and energetic of the primary photochemistry of photosystem II of oxygenic photosynthesis, Annu. Rev. Plant Biol. 53 (2002) 551–580.
[4] J.-R. Shen, Structure of photosystem II and the mechanism of water oxidation in photosynthesis, Annu. Rev. Plant Biol. 66 (2015) 23–48.
[5] M. Pérez-Navarro, F. Neese, W. Lubitz, D.A. Pantazis, N. Cox, Recent developments in biological water oxidation, Curr. Opin. Chem. Biol. 31 (2016) 113–119.
[6] B. Kok, B. Forbush, M. McGloin, Cooperation of charges in photosynthetic O_2 evolution–I. A linear four step mechanism, Photochem. Photobiol. 11 (1970) 457–475.
[7] Oxygen evolution in photosynthesis, in: P. Joliot, B. Kok, Govindjee (Eds.), Bioenergetics of Photosynthesis, Academic Press, New York 1975, pp. 387–412.
[8] N. Cox, J. Messinger, Reflections on substrate water and dioxygen formation, Biochim. Biophys. Acta 1827 (2013) 1020–1030.
[9] J. Yano, V. Yachandra, Mn_4Ca cluster in photosynthesis: where and how water is oxidized to dioxygen, Chem. Rev. 114 (2014) 4175–4205.
[10] B.A. Diner, E. Schlodder, P.J. Nixon, W.J. Coleman, F. Rappaport, J. Lavergne, W.F. Vermaas, D.A. Chisholm, Site-directed mutations at D1-His198 and D2-His197 of photosystem II in *Synechocystis PCC 6803*: sites of primary charge separation and cation and triplet stabilization, Biochemistry 40 (2001) 9265–9281.
[11] E. Romero, B.A. Diner, P.J. Nixon, W.J. Coleman, J.P. Dekker, R. van Grondelle, Mixed exciton–charge-transfer states in photosystem II: stark spectroscopy on site-directed mutants, Biophys. J. 103 (2012) 185–194.
[12] K. Saito, T. Ishida, M. Sugiura, K. Kawakami, Y. Umena, N. Kamiya, J.-R. Shen, H. Ishikita, Distribution of the cationic state over the chlorophyll pair of the photosystem II reaction center, J. Am. Chem. Soc. 133 (2011) 14379–14388.
[13] F. Rappaport, B.A. Diner, Primary photochemistry and energetics leading to the oxidation of the Mn4Ca cluster and to the evolution of molecular oxygen in photosystem II, Coord. Chem. Rev. 252 (2008) 259–272.
[14] J.P. Allen, K. Artz, X. Lin, J.C. Williams, A. Ivancich, D. Albouy, T.A. Mattioli, A. Fetsch, M. Kuhn, W. Lubitz, Effects of hydrogen bonding to a bacteriochlorophyll-bacteriopheophytin dimer in reaction centers from Rhodobacter-sphaeroides, Biochemistry 35 (1996) 6612–6619.
[15] X. Lin, H.A. Murchison, V. Nagarajan, W.W. Parson, J.P. Allen, J.C. Williams, Specific alteration of the oxidation potential of the electron donor in reaction centers from Rhodobacter sphaeroides, Proc. Natl. Acad. Sci. U. S. A. 91 (1994) 1026510269.
[16] K. Saito, J.-R. Shen, H. Ishikita, Influence of the axial ligand on the cationic properties of the chlorophyll pair in photosystem II from *Thermosynechococcus vulcanus*, Biophys. J. 102 (2012) 2634–2640.
[17] F. Rappaport, M. Guergova-Kuras, P.J. Nixon, B.A. Diner, J. Lavergne, Kinetics and pathways of charge recombination in photosystem II, Biochemistry 41 (2002) 8518–8527.
[18] H. Ishikita, W. Saenger, J. Biesiadka, B. Loll, E.W. Knapp, How photosynthetic reaction centers control oxidation power in chlorophyll pairs P680, P700, and P870, Proc. Natl. Acad. Sci. U. S. A. 103 (2006) 9855–9860.
[19] N. Ginet, J. Lavergne, Interactions between the donor and acceptor sides in bacterial reaction centers, Biochemistry 39 (2000) 16252–16262.
[20] J. Alric, A. Cuni, H. Maki, K.V. Nagashima, A. Vermeglio, F. Rappaport, Electrostatic interaction between redox cofactors in photosynthetic reaction centers, J. Biol. Chem. 279 (2004) 47849–47855.
[21] H. Ishikita, B. Loll, J. Biesiadka, W. Saenger, E.W. Knapp, Redox potentials of chlorophylls in the photosystem II reaction center, Biochemistry 44 (2005) 4118–4124.
[22] K. Hasegawa, T. Noguchi, Density functional theory calculations on the dielectric constant dependence of the oxidation potential of chlorophyll: implication for the high potential of P680 in photosystem II, Biochemistry 44 (2005) 8865–8872.
[23] J. Fajer, Chlorophyll chemistry before and after crystals of photosynthetic reaction centers, Photosynth. Res. 80 (2004) 165–172.
[24] M. Sugiura, A. Boussac, T. Noguchi, F. Rappaport, Influence of Histidine-198 of the D1 subunit on the properties of the primary electron donor, P680, of photosystem II in *Thermosynechococcus elongatus*, Biochim. Biophys. Acta 1777 (2008) 331–342.
[25] J.L. Hughes, N. Cox, A.W. Rutherford, E. Krausz, T.–.L. Lai, A. Boussac, M. Sugiura, D1 protein variants in photosystem II from *Thermosynechococcus elongatus* studied by low temperature optical spectroscopy, Biochim. Biophys. Acta 1797 (2010) 11–19.
[26] Y. Shibuya, R. Takahashi, T. Okubo, H. Suzuki, M. Sugiura, T. Noguchi, Hydrogen bond interaction of the pheophytin electron acceptor and its radical anion in photosystem II as revealed by Fourier transform infrared difference spectroscopy, Biochemistry 49 (2010) 493–501.
[27] M. Sugiura, Y. Inoue, Highly purified thermo-stable oxygen-evolving photosystem II core complex from the thermophilic cyanobacterium *Synechococcus elongatus* having His-tagged CP43, Plant Cell Physiol. 40 (1999) 1219–1231.
[28] M. Sugiura, C. Azami, K. Koyama, A.W. Rutherford, F. Rappaport, A. Boussac, Modification of the pheophytin redox potential in *Thermosynechococcus elongatus* photosystem II with PsbA3 as D1, Biochim. Biophys. Acta 1837 (2014) 139–148.
[29] D. Beal, F. Rappaport, P. Joliot, A new high–sensitivity 10–ns time–resolution spectrophotometric technique adapted to in vivo analysis of the photosynthetic apparatus, Rev. Sci. Instrum. 70 (1999) 202–207.
[30] J.-M. Ducruet, Chlorophyll thermoluminescence of leaf discs: simple instruments and progress in signal interpretation open the way to new ecophysiological indicators, J. Exp. Bot. 54 (2003) 2419–2430.
[31] J.–.M. Ducruet, I. Vass, Thermoluminescence: experimental, Photosynth. Res. 201 (2009) 195–204.
[32] C. Fufezan, C.-X. Zhang, A. Krieger-Liszkay, A.W. Rutherford, Secondary quinone in photosystem II of *Thermosynechococcus elongatus*: semiquinone-iron EPR signals and temperature dependence of electron transfer, Biochemistry 44 (2005) 12780–12789.
[33] A.W. Rutherford, Y. Govindjee, Inoue, charge accumulation and photochemistry in leaves studied by thermolumiscence and delayed light-emission, Proc. Natl. Acad. Sci. U. S. A. 81 (1984) 1107–1111.
[34] F. Rappaport, A. Cuni, L. Xiong, R. Sayre, J. Lavergne, Charge recombination and thermoluminescence in photosystem II, Biophys. J. 88 (2005) 1948–1958.
[35] K. Cser, I. Vass, Radiative and non–radiative charge recombination pathways in photosystem II studied by thermoluminescence and chlorophyll fluorescence in the cyanobacterium *Synechocystis* 6803, Biochim. Biophys. Acta 1767 (2007) 233–243.
[36] F. Rappaport, J. Lavergne, Thermoluminescence: theory, Photosynth. Res. 101 (2009) 205–216.
[37] S.A.P. Merry, P.J. Nixon, L.M.C. Barter, M. Schilstra, G. Porter, J. Barber, J.R. Durrant, D.R. Klug, Modulation of quantum yield of primary radical pair formation in photosystem II by site–directed mutagenesis affecting radical cations and anions, Biochemistry 37 (1998) 17439–17447.